

Table 1. ^1H NMR (CD_3OD , 500 MHz) and ^{13}C NMR (CD_3OD , 125 MHz) Data for Alkaloids 2 and 3

position	2^a		3^b	
	δ_{C} , type	δ_{H} (J in Hz)	δ_{C} , type	δ_{H} (J in Hz)
2	144.5, C		147.4, C	
3	142.2, C		139.1, C	
4	174.3, C		174.1, C	
4a	121.1, C		121.0, C	
5	142.6, C		143.8, C	
6	141.4, C		141.4, C	
7	124.5, CH	7.03, d (8.0)	127.8, CH	7.44, d (8.0)
8	118.3, CH	7.35, d (8.0)	118.7, CH	7.49, d (8.0)
8a	139.7, C		139.9, C	
9	86.6, C		89.0, C	
10	32.8, CH_2	2.12, m	69.6, CH	4.27, dd (9.5, 6.0)
11	18.6, CH_2	1.00, 1.63, m	27.7, CH_2	0.74, 1.88, m
12	26.7, CH_2	1.86, 2.02, m	28.8, CH_2	1.90, 2.10, m
13	81.3, CH	6.30, d (2.5)	80.7, CH	6.17, d (2.0)
1'	143.4, C		140.4, C	
2'	126.9, CH	7.51, d (8.0)	129.1, CH	7.71, d (8.0)
3'	129.1, CH	7.37, t (8.0)	129.1, CH	7.39, t (7.5)
4'	128.6, CH	7.30, t (8.0)	129.1, CH	7.33, t (8.0)
5'	129.1, CH	7.37, t (8.0)	129.1, CH	7.39, t (7.5)
6'	126.9, CH	7.51, d (8.0)	129.1, CH	7.71, d (8.0)
1''			107.6, CH	4.68, d (7.0)
2''			75.5, CH	3.46, m
3''			78.5, CH	3.32 ^c
4''			71.2, CH	3.42, m
5''			78.6, CH	3.28 ^c
6''			62.6, CH_2	3.70, dd (12.0, 5.5)
3.86, brd (12.0)				
OCH_3 (3)	60.4	3.82, s		
CH_3 (2)	14.6	2.46, s	15.9, CH_3	2.61, s

^aMeasured in CD_3OD and CDCl_3 . ^bMeasured in CD_3OD . ^cSignal obscured by the CD_3OD solvent peak.

6') exhibiting the expected symmetry. The other major structural difference between alkaloids 1 and 2 is the loss of oxygenation of C-10 in 2 as evident from the loss of the signal at δ_{H} 4.73 and the presence of an additional methylene signal at δ_{H} 2.10 (H_2 -10). Finally, the HMBC correlation between C-9 and H-13 indicated an ether bridge connecting C-9 to C-13. The change in the coupling constant of the doublet signal of H-13 from $J = 6.5$ Hz in 1 to $J = 2.0$ Hz in 2 gave additional proof to this change from a five-membered fused ether ring encompassing C-10 to C-13 in 1 to a six-membered fused ether ring encompassing C-9 to C-13 in 2. Additionally, C-9 showed HMBC correlations with the aromatic protons H-2'/H-6' and with H-7. Other relevant HMBC correlations are shown in Figure 1. Correlations in the COSY spectra showed the vicinal connectivities of H-10, H_2 -11, H_2 -12, and H-13 (Figure 1).

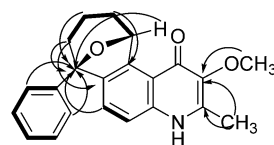


Figure 1. Key COSY (solid lines) and HMBC (arrows) correlations in alkaloid 2.

The bicyclic ring system in 2 is geometrically constrained to have the 4-quinolone moiety fused to the tetrahydropyran ring in a 1,3-diaxial arrangement. This places both the phenyl and hydrogen substituents at C-9 and C-13, respectively, equatorial with respect to the tetrahydropyran ring. Thus, H-13 exhibited similar magnitude NOE interactions to both diastereotopic hydrogens H_2 -14, suggesting a chair conformation for the tetrahydropyran ring.

Waltherione D (3) was isolated as an off-white powder. The molecular formula, $\text{C}_{27}\text{H}_{30}\text{NO}_9$, was deduced from the HRESIMS ($[\text{M} + \text{H}]^+$ at m/z 512.1930, calcd 512.1921). Waltherione D is the 3-*O*-demethyl- β -glycosylated, 10-hydroxylated analogue of alkaloid 2. The ^{13}C and ^1H NMR data of 3 were found to be more similar to 2 than to 1 (Table 1). There was, however, a loss in 3 of a signal of a methoxy group attached to C-3 in both 1 and 2. Instead, a glucose residue was attached to the oxygen of C-3. The presence of glucose was evident from the ESIMS, which showed an in-source fragment ion at m/z 350 ($[\text{M} + \text{H} - 162]^+$), and can be explained by the loss of the glucosyl moiety. This was confirmed by acid hydrolysis of alkaloid 3 and analysis of the sugar fraction by TLC and polarimetry. Co-elution on TLC of the aqueous extract from the acid hydrolysis with an authentic D-glucose sample proved that the sugar residue is glucose. The positive optical activity of this aqueous extract proved that the glucosyl group has the D-configuration. The position of the glucosyl moiety was established from the HMBC spectra of 3 showing a correlation between the anomeric proton H-1'' and C-3 (Figure 2). An NOE between H-1'' and the methyl protons

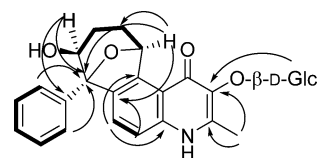


Figure 2. Key COSY (solid lines) and HMBC (arrows) correlations in alkaloid 3.

attached to C-2 was also observed from the ROESY spectrum (Figure 3B). The glucose residue was in an *O*- β -glycosidic linkage, as evident from the coupling constant of H-1'' to H-2'' ($J = 7$ Hz), indicating that H-1'' is in the axial position. In addition, ROESY correlations were observed from H-1'' to both

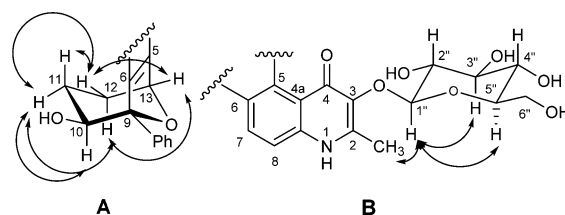


Figure 3. Key NOESY correlations in alkaloid 3.

H-3" and H-5", consistent with an *O*- β -glucosyl residue (Figure 3B). Relevant HMBC correlations are shown in Figure 2.

Position C-10 in alkaloid **3** is oxygenated as in **1**. However, **3** has the same six-membered fused ether ring encompassing C-9 to C-13 as in **2**. This was determined from the HMBC correlation between H-13 and C-9 (Figure 2). The relative configuration of **3** was deduced from the ^1H NMR and ROESY data. The six-membered tetrahydropyran ring of C-9 to C-13 appears to adopt a chair conformation to which the aromatic ring of the quinolone system is fused diaxially (Figure 3A) as in **2**. Also as in **2**, both the phenyl and hydrogen substituents to C-9 and C-13, respectively, are equatorial with respect to the tetrahydropyran ring. H-13 was hence observed as a doublet with $J = 2$ Hz, proving its equatorial orientation. H-10 on the other hand, was seen to be in the axial position due to its double doublet signal with $J = 9.5$ Hz and $J = 6$ Hz, corresponding to its coupling with H-11_{ax} and with H-11_{eq}, respectively. A cross-peak in the ROESY spectrum showed an NOE between axial H-10 and H-2'/H-6' of the equatorial phenyl ring, suggesting that H-10 and the aromatic ring are gauche to one another (Figure 3A). Additional data from the ROESY spectra confirmed the proposed chair conformation; namely, H-10 (δ_{H} 4.27) showed a correlation with H-11_{eq} (δ_{H} 1.88) but not with H-11_{ax} (δ_{H} 0.74); H-11_{ax} exhibited a correlation with H-12_{eq} (δ_{H} 1.90) but not with H-12_{ax} (δ_{H} 2.10); and H-13 showed two correlations with H-12_{eq} and H-12_{ax} of equal intensity (Figure 3A). It was not possible to relate the relative configuration of the sugar moiety to the bicyclic ether, and thus the relative configurations depicted in the structural diagram of **3** for the corresponding groups are independent of one another.

Two of the alkaloids, waltheriones A (**1**) and C (**2**), showed significant cytoprotection⁴ against HIV-1 in infected CEM-TART cells in vitro (Table 2). A second assay measuring the

significant activity. It would seem that the methoxy group at C-3, the site of glycosylation in **3**, and the bicyclic ring system fused to a 4-quinolone ring are important determinants of the anti-HIV activity of the waltheriones. The shift in the ether bridgehead of the bicyclic ring system from C-10 to C-9 seems to marginally enhance anti-HIV activity and decrease toxicity, as seen from the greater efficacy of **2** compared with **1**. The methoxy group at C-2' does not seem to be important for anti-HIV activity since **2**, which does not have this functional group, exhibited activity in both cytoprotection and P24 inhibition assays. The waltheriones represent a structurally distinct class from both the HIV integrase inhibitory and the HIV reverse transcriptase inhibitory classes of 4-quinolones. Further work on these alkaloids may improve our understanding of the structure–activity relationship of the anti-HIV activity of the waltheriones.

EXPERIMENTAL SECTION

General Experimental Procedures. Specific rotations were recorded on a Perkin-Elmer (Downers Grove, IL, USA) 343 digital polarimeter in MeOH at 22 °C. UV spectra were measured on a Hewlett-Packard 8452A diode array spectrophotometer (Agilent, Santa Clara, CA, USA). IR spectra were recorded using a JASCO (Easton, MD, USA) FT/IR-400 spectrometer. NMR spectra were recorded on a Varian (Palo Alto, CA, USA) INOVA at 500 MHz for ^1H and 125 MHz for ^{13}C using vendor-supplied pulse sequences. Residual solvent (CD_3OD) signals were used as reference (δ_{H} 3.31; δ_{C} 49.2). Accurate mass measurements were performed by HRESIMS on a Micromass Q-tof Micro (Waters, MA, USA), using the positive-ion mode, and a FTMS (LTQ-FT, ThermoFisher, Waltham, MA, USA). HPLC was performed on an Agilent 1200 series equipped with PDA detector (Agilent Technologies, Santa Clara, CA, USA). A Luna 5 μm , 250 \times 10 mm C_{18} column (Phenomenex, Torrance, CA, USA) was used for the isolation of the three alkaloids. Supelco Diaion HP20SS was purchased from Sigma-Aldrich (St. Louis, MO, USA). TLC was conducted using Kieselgel 60 F₂₅₄ (Merck, Whitehouse Station, NJ, USA).

Plant Material. Stems and twigs of *Melochia odorata* were collected near Pauluaku Village, Buin District, Autonomous Regions of Bougainville, Papua New Guinea, in January 2004, as previously described,¹⁶ as part of an ICBG agreement. Voucher specimens (U20246-180) have been deposited at the University of PNG Herbarium, Port Moresby, and the PNG Forest Research Institute, Lae, PNG, and the plant was identified by two of the authors (O.G.G. and P.P.).

Extraction and Isolation. Air-dried stems and twigs (30.0 g) of *M. odorata* were ground and extracted with 500 mL of MeOH (2 \times 24 h). The crude methanol extract (2.8 g) was dissolved in MeOH and mixed with 8.4 g of Diaion HP20SS and dried. The resin was loaded into a column (8.5 cm \times 2.0 cm i.d.) and fractionated using 40 mL each of the following solvents: 100% water, 75% H_2O /25% 2-propanol, 50% H_2O /50% 2-propanol, 25% H_2O /75% 2-propanol, and 100% MeOH to yield five fractions, designated FW, F1, F2, F3, and F4.¹⁷ The fractions were collected and solvents evaporated using a rotary evaporator.

Bioassay-guided fractionation showed cytoprotective anti-HIV activity for F1 (0.205 g) and F2 (0.196 g). Fraction 2 was found to be the more potent protector of T cells against HIV-mediated lysis at 10 $\mu\text{g}/\text{mL}$ ($p < 0.005$), while not displaying cytotoxicity to human T cells below 50 $\mu\text{g}/\text{mL}$. F2 was fractionated by semipreparative HPLC using a reversed-phase C_{18} column employing the following method at 3.5 mL/min flow rate: 30% methanol/70% water from 0 to 5 min and linear gradient from 30% to 100% methanol from 5 to 30 min. Compound **3** (2.4 mg) eluted at 14.7 min, compound **1** (1.4 mg) at 20.8 min, and compound **2** (2.4 mg) at 25.3 min.

Additional material for the acid hydrolysis and determination of the absolute configuration of the monosaccharide in alkaloid **3** was obtained from F1. F1 (0.205 g) was separated by Sephadex LH-20

Table 2. Cytoprotection and Toxicity Assay Data of Alkaloids 1–3

alkaloid	cytoprotection EC_{50} (μM) ^a [standard deviation]	cytotoxicity LC_{50} (μM) ^b [standard deviation]
1	56.2 [12.3]	102 [2.25]
2	0.84 [0.8]	11 [1.36]
3	not effective ^c	not toxic ^c
AZT	1.30 [0.12]	89.5 [10.8]

^aProtection of CEM-TART cells from killing by HIV infection at 96 h (EC_{50}). ^bSurvival was measured by MTT metabolism by viable cells (LC_{50}). ^cNot effective or toxic at the highest concentration tested (100 μM).

production of HIV capsid protein P24¹⁵ in infected T cells confirmed the anti-HIV activity of **1** and **2** (Figures 4 and 5), showing >50% inhibition at 1.7 and 0.95 μM , respectively. Each of these anti-HIV assays also provides secondary outcome measures of cytotoxicity. While no significant toxicity was observed with alkaloids 1–3 in the 48 h P24 assay, narrower therapeutic indices were observed in the 96 h cytoprotection assay (Table 2). To quantify these theoretical therapeutic indices, the MTT cytotoxicity assay (determined at approximately 72 h) was performed. The $\text{EC}_{50}/\text{LC}_{50}$ ratio for **1** was approximately 2; for compound **2** it was a more promising 13-fold.

Alkaloids **1** and **2** showed in vitro anti-HIV activity, with **2** showing less toxicity than **1**. Alkaloid **3** did not show any

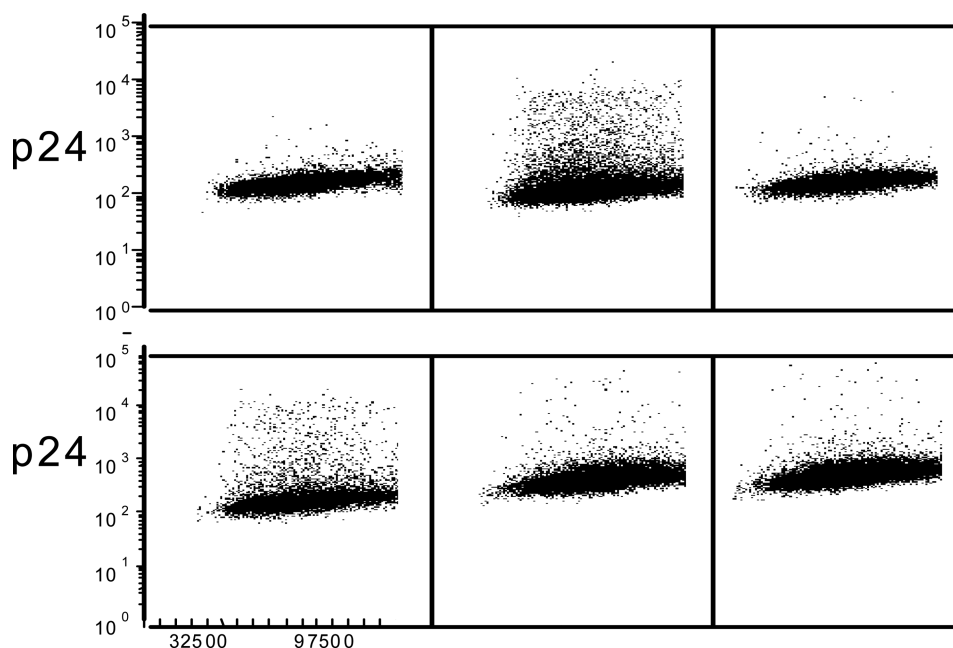


Figure 4. P24 production assay results \pm HIV and 1–3 in CEM-TART cells at 48 h. Abscissa: cell size as measured by forward scatter; ordinate: intracellular indirect immunofluorescent staining of HIV capsid protein P24 via FITC (see methods). Top row, left to right: control, HIV infected, AZT treated (5 μ g/mL). Bottom row, left to right: 3, 1, and 2 at 5 μ g/mL.

Waltherione Protection from HIV Infection at 48 Hours

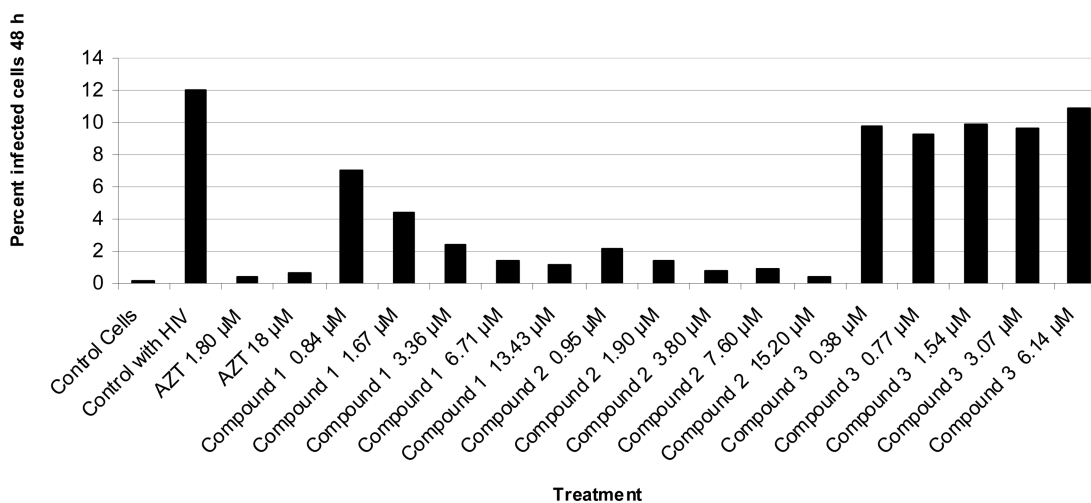


Figure 5. Dose-dependent inhibition of P24 production by AZT and waltheriones in CEM-TART cells at 48 h. P24 production was measured by indirect immunofluorescent staining of HIV P24.

(MeOH) chromatography, affording four fractions: F1-1 to F1-4. F1-2 (77 mg) was purified by semipreparative HPLC using the same method described above for F2 to yield 3.5 mg of **3**.

Waltherione C (2): off-white solid; $[\alpha]_D^{22}$ -17.0 (c 0.15, MeOH); UV (MeOH) λ_{\max} nm ($\log \epsilon$) 212 (3.08), 246 (3.14), 334 (2.53), 348 (2.52) nm; IR (NaCl disk) ν_{\max} 3392, 2924, 2360, 1634, 1560, 1508, 1022 cm^{-1} ; ^1H NMR (CD_3OD , 500 MHz) and ^{13}C NMR (CD_3OD , 125 MHz) see Table 1; HRESIMS m/z 348.1600 $[\text{M} + \text{H}]^+$ (calcd for $\text{C}_{22}\text{H}_{22}\text{NO}_3$ 348.15942; Δ +2.0 ppm).

Waltherione D (3): off-white solid; $[\alpha]_D^{22}$ -30.8 (c 0.12, MeOH); UV (MeOH) λ_{\max} nm ($\log \epsilon$) 212 (3.68), 238 (3.47), 282 (2.91), 330 (2.78), 344 (2.72) nm; IR (NaCl disk) ν_{\max} 3400, 2928, 1631, 1604, 1563, 1513, 1272 cm^{-1} ; ^1H NMR (CD_3OD , 500 MHz) and ^{13}C NMR (CD_3OD , 125 MHz) see Table 1; ESIMS positive mode m/z 512 $[\text{M} + \text{H}]^+$, 350 $[\text{M} + \text{H} - 162]^+$; HRESIMS m/z 512.1930 $[\text{M} + \text{H}]^+$ (calcd for $\text{C}_{27}\text{H}_{30}\text{NO}_9$ 512.1921; Δ +1.8 ppm).

Acid Hydrolysis of 3. A solution of alkaloid **3** (2.0 mg) with a mixture of concentrated HCl (0.5 mL), H_2O (1.5 mL), and dioxane (3.0 mL) was refluxed on a boiling water bath for 2 h.¹⁸ After the completion of the reaction [monitored by following the disappearance of **3** on TLC (CHCl_3 –MeOH, 8:2) detected by UV], the reaction mixture was extracted with ethyl acetate (3×5 mL). The aqueous layer was neutralized with 5% NaHCO_3 , concentrated to dryness under reduced pressure, and purified by Sephadex LH-20 chromatography (MeOH) to give a sugar fraction. The sugar (0.7 mg) was confirmed as D-glucose by comparison with an authentic sample on TLC [CHCl_3 /MeOH/ H_2O (8:5:1), R_f 0.3, detected by spraying with anisaldehyde/MeOH/ H_2SO_4 (0.5:0.5:9) spray reagent followed by heating] and measurement of its optical rotation ($[\alpha]_D^{20}$ +43.5, c 0.023, H_2O).

Cytoprotective HIV Assay. 1A2 cells (a subclone of CEM-TART cells⁴ that are more sensitive to lysis upon HIV infection) were

cultured in RPMI 1640/20% FBS and plated in 96-well plates.⁵ Controls included DMSO-treated cells without HIV, DMSO-treated cells infected with HIV, and cells infected with HIV and treated with azidothymidine (AZT) at final concentrations of 5 or 0.5 $\mu\text{g}/\text{mL}$.⁵ Treatment of control cells with DMSO or drug-treated cells with DMSO/drug (1% vol) was delayed 2 h after infection with HIV stock. This delay reduces the detection of entry-inhibitor drugs and promotes detection of drugs that protect T cells from HIV killing by intracellular mechanisms.¹⁹ Uninfected and HIV-infected cells were allowed to incubate for 96 h at 37 °C in 5% CO₂, at which time cell viability was assessed with a standard MTT assay, initiated by the addition of 11 $\mu\text{L}/\text{well}$ of 5 mg/mL MTT in PBS to each culture well. To solubilize the formazan precipitate after 3 to 4 h of further incubation, cells were pelleted, the medium was aspirated, and 100 μL of DMSO/0.1% SDS was added.²⁰ Plates were read on a Fisher Scientific Multiskan FC (Fisher Scientific, Waltham, MA, USA) plate reader at 570 nm absorbance. On each assay plate, each condition was performed in triplicate and *p* values were determined between groups to gauge the performance of the assay. For a compound or extract to be considered active in the screen it must rescue at least 50% as many infected cells as the more protective of the two AZT positive controls and must provide statistically significant (*p* < 0.05) better survival than untreated control HIV-infected cells.⁵ To calculate EC₅₀ (effective concentration of a compound to achieve 50% of the protection afforded by 5 μM AZT) and LC₅₀ (concentration exhibiting 50% cell killing in HIV uninfected 1A2 cells), dose response experiments and standards of deviation¹⁶ and standards of deviation data from multiple experiments (≥ 3) were combined and analyzed using EDS0plus V1.0 (mhvargas@conacyt.mx).

P24 Inhibition Assay. Controls included cells without HIV, cells infected with HIV, and cells infected with HIV and treated with AZT at final concentrations of 5 or 0.5 $\mu\text{g}/\text{mL}$. Control and extract-treated cells were washed twice in PBS and incubated at 1:100 with murine myeloma IgG (m5284, Sigma-Aldrich) in PBS for 30 min at 4 °C. Cells were then washed in PBS, fixed in PBS/1% paraformaldehyde/0.05% Triton X100, washed in FACS buffer (PBS, 2.0% FBS, 0.05% Triton X100), and exposed to 1:50 dilution of AG3.0 mouse monoclonal²¹ anti-P24 antibody in FACS buffer for 30 min at 4 °C.¹⁵

The antibody-treated cells were washed twice in FACS buffer and exposed to goat-anti-mouse FITC conjugated secondary antibody for 30 min at 4 °C, washed twice in FACS buffer, and analyzed on a BD FACSCanto instrument (BD Bioscience San Jose, CA, USA) (Figure 3).

Cytotoxicity Assay. Cytotoxicity was determined in a 3-(4,5-dimethylthiazol-2-yl)-2,5-diphenyltetrazolium bromide (MTT) assay.⁵ Drugs were dissolved in DMSO at the required concentrations; the final concentration of DMSO was 0.5%. Drugs and 20 000 CEM-TART cells were seeded in 96-well plates in fresh RPMI medium supplemented with 20% FBS and antibiotic and allowed to incubate at 37 °C in a 5% CO₂ atmosphere for 72 h, after which 11 μL of MTT (5 mg/mL in PBS) was added. Viable cells reduce MTT to a purple formazan product that was solubilized in DMSO/0.1% SDS and quantified on a plate reader as described above. Tests were performed in triplicate or quadruplicate.

■ ASSOCIATED CONTENT

📄 Supporting Information

¹H and ¹³C NMR spectra of compounds 2 and 3 are available. This material is available free of charge via the Internet at <http://pubs.acs.org>.

■ AUTHOR INFORMATION

Corresponding Author

*Tel: 801 582 4547. Fax: 801 585 5111. E-mail: lbarrows@pharm.utah.edu.

Notes

The authors declare no competing financial interest.

■ ACKNOWLEDGMENTS

The authors wish to gratefully acknowledge NIH support through the ICBG SU01TW006671-3. The following reagent was obtained through the NIH AIDS Reagent Program, Division of AIDS, NIAID, NIH: CEM-TART from Drs. H. Chen, T. Boyle, M. Malim, B. Cullen, and H. K. Lyerly; and monoclonal antibody to HIV-1 p24 (AG3.0) from Dr. J. Allan.

■ REFERENCES

- (1) Ahmed, A.; Daneshtalab, M. *J. Pharm. Pharmaceut. Sci.* **2012**, *15*, 52–72.
- (2) Di Santo, R.; Costi, R.; Roux, A.; Artico, M.; Lavecchia, A.; Marinelli, L.; Novellino, E.; Palmisano, L.; Andreotti, M.; Amici, R.; Galluzzo, C. M.; Nencioni, L.; Palamara, A. T.; Pommier, Y.; Marchand, C. *J. Med. Chem.* **2006**, *49*, 1939–1945.
- (3) Cheng, P.; Gu, Q.; Liu, W.; Zou, J. F.; Ou, Y. Y.; Lou, Z. Y.; Zeng, J. *G. Molecules* **2011**, *16*, 7649–7661.
- (4) Kiser, R.; Makovsky, S.; Terpening, S. J.; Laing, N.; Clanton, D. J. *J. Virol. Methods* **1996**, *58*, 99–109.
- (5) Lu, Z.; Harper, M. K.; Pond, C. D.; Barrows, L. R.; Ireland, C. M.; Van Wagoner, R. M. *J. Nat. Prod.* **2012**, *75*, 1436–1440.
- (6) Hoelzel, S. C. S. M.; Vieira, E. R.; Giacomelli, S. R.; Dalcol, I. I.; Zanatta, N.; Morel, A. F. *Phytochemistry* **2005**, *66*, 1163–1167.
- (7) Gressler, V.; Stücker, C. Z.; Dias, G. O. C.; Dalcol, I. I.; Burrow, R. A.; Schmidt, J.; Wessjohann, L.; Morel, A. F. *Phytochemistry* **2008**, *69*, 994–999.
- (8) Dias, G. O. C.; Gressler, V.; Hoelzel, S. C. S. M.; Silva, U. F.; Dalcol, I. I.; Morel, A. F. *Phytochemistry* **2007**, *68*, 668–672.
- (9) Emile, A.; Waikedre, J.; Herrenknecht, C.; Fourneau, C.; Gantier, J.-C.; Hnawia, E.; Cabalion, P.; Hocquemiller, R.; Fournet, A. *Phytother. Res.* **2007**, *21*, 398–400.
- (10) Lima, M. M. C.; Lopez, J. A.; David, J. M.; Silva, E. P.; Giulietti, A. M.; de Queiroz, L. P.; David, J. P. *Planta Med.* **2009**, *75*, 335–337.
- (11) Buske, A.; Schmidt, J.; Hoffmann, P. *Phytochemistry* **2002**, *60*, 489–496.
- (12) Dias, G. O. C.; Porto, C.; Stücker, C. Z.; Graessler, V.; Burrow, R. A.; Dalcol, I. I.; da Silva, U. F.; Morel, A. F. *Planta Med.* **2007**, *73*, 289–292.
- (13) Kapadia, G. J.; Paul, B. D.; Silvertown, J. V.; Fales, H. M.; Sokoloski, E. A. *J. Am. Chem. Soc.* **1975**, *97*, 6814–6819.
- (14) Warurai, J.; Sipana, B.; Koch, M.; Barrows, L. R.; Maitanaho, T. K.; Rai, P. P. *J. Ethnopharmacol.* **2011**, *138*, 564–577.
- (15) Spector, S. A.; Kennedy, C.; McCutchan, J. A.; Bozzette, S. A.; Straube, R. G.; Connor, J. D.; Richman, D. D. *J. Infect. Dis.* **1989**, *159*, 822–828.
- (16) Judulco, R. C.; Koch, M.; Van Wagoner, R. M.; Pond, C.; Gideon, O. G.; Maitanaho, T.; Piskaut, P.; Barrows, L. R. *Planta Med.* **2011**, *77*, 1651–1654.
- (17) Bugni, T. S.; Harper, M. K.; McCulloch, M. W. B.; Reppart, J.; Ireland, C. M. *Molecules* **2008**, *13*, 1372–1383.
- (18) Yuan, T.; Wan, C.; González-Sarrias, A.; Kandhi, V.; Cech, N. B.; Seeram, N. P. *J. Nat. Prod.* **2011**, *74*, 2472–2476.
- (19) Andjelic, C. D.; Planelles, V.; Barrows, L. R. *Mar. Drugs* **2008**, *6*, 528–549.
- (20) Howett, M. K.; Neely, E. B.; Christensen, N. D.; Wigdahl, B.; Krebs, F. C.; Malamud, D.; Patrick, S. D.; Pickel, M. J.; Welsh, P. A.; Reed, C. A.; Ward, M. G.; Budgeon, L. R.; Kreider, J. W. *Antimicrob. Agents Chemother.* **1999**, *43*, 314–321.
- (21) Sanders-Beer, B. E.; Eschricht, M.; Seifried, J.; Hirsch, V. M.; Allan, J. S.; Norley, S. *Virology* **2012**, *422*, 402–412.